Refractive elements for the measurement of the orbital angular momentum of a single photon

Martin P. J. Lavery,[1,*] David J. Robertson,[2] Gregorius C. G. Berkhout,[3] Gordon D. Love,[2] Miles J. Padgett,[1] and Johannes Courtial[1]

[1]*School of Physics and Astronomy, University of Glasgow, Glasgow, G12 8QQ, UK*
[2]*Centre for Advanced Instrumentation, Durham University, Durham, DH1 3LE, UK*
[3]*Huygens Laboratory, Leiden University, P.O. Box 9504, 2300 RA Leiden, The Netherlands*
[*]*m.lavery@physics.gla.ac.uk*

Abstract: We have developed a mode transformer comprising two custom refractive optical elements which convert orbital angular momentum states into transverse momentum states. This transformation allows for an efficient measurement of the orbital angular momentum content of an input light beam. We characterise the channel capacity of the system for 50 input modes, giving a maximum value of 3.46 bits per photon. Using an electron multiplying CCD (EMCCD) camera with a laser source attenuated such that on average there is less than one photon present within the system per measurement period, we demonstrate that the elements are efficient for the use in single photon experiments.

OCIS codes: (060.4510) Optical communications; (050.4865) Optical vortices; (060.5565) Quantum communications; (080.3630) Lenses.

References and links

1. L. Allen, M. Beijersbergen, R. Spreeuw, and J. Woerdman, "Orbital angular momentum of light and the transformation of Laguerre-Gaussian laser modes," Phys. Rev. A **45**, 8185–8189 (1992).
2. A. M. Yao and M. J. Padgett, "Orbital angular momentum: origins, behavior and applications," Adv. Opt. Photon. **3**, 161–204 (2011).
3. G. Molina-Terriza, J. P. Torres, and L. Torner, "Twisted photons," Phys. Rev. Lett. **88**, 013601 (2001).
4. A. Vaziri, G. Weihs and A. Zeilinger, "Experimental two-photon, three-dimensional entanglement for quantum communication," Phys. Rev. Lett. **89**, 240401 (2002).
5. G. Gibson, J. Courtial, M. Padgett, M. Vasnetsov, V. Pas'ko, S. Barnett, and S. Franke-Arnold, "Free-space information transfer using light beams carrying orbital angular momentum," Opt. Express **12**, 5448–5456 (2004).
6. J. T. Barreiro, T. C. Wei, and P. G. Kwiat, "Beating the channel capacity limit for linear photonic superdense coding," Nat. Phys. **4**, 282 (2008).
7. J. Leach, B. Jack, J. Romero, A. K. Jha, A. M. Yao, S. Franke-Arnold, D. G. Ireland, R. W. Boyd, S. M. Barnett, M. J. Padgett, "Quantum correlations in optical angle-orbital angular momentum variables," Science **329**, 662–655 (2010).
8. V. Bazhenov, M. Soskin, and M. Vasnetsov, "Screw dislocations in light wave-fronts," J. Mod. Opt. **39**, 985–990 (1992).
9. N. Heckenberg, R. McDuff, C. Smith, and A. White, "Generation of optical phase singularities by computer-generated holograms," Opt. Lett. **17**, 221–223 (1992).
10. A. Mair, A. Vaziri, G. Weihs, and A. Zeilinger, "Entanglement of the orbital angular momentum states of photons," Nature **412**, 313–316, (2001).
11. S. S. Oemrawsingh, J. de Jong, X. Ma, and A. Aiello. "High- dimensional mode analyzers for spatial quantum entanglement, Phys. Rev. A **73**, 032339, (2006)

#153707 - $15.00 USD Received 1 Sep 2011; revised 10 Nov 2011; accepted 2 Dec 2011; published 17 Jan 2012

12. L. Marrucci, E. Karimi, S. Slussarenko, B, Piccirillo, E. Santamato, E. Nagali and F. Sciarrino, "Spin-to-orbital conversion of the angular momentum of light and its classical and quantum applications," J. Opt. **13**, 064001, (2011).
13. J. Leach, M. Padgett, S. Barnett, S. Franke-Arnold, and J. Courtial, "Measuring the orbital angular momentum of a single photon," Phys. Rev. Lett. **88**(25), 257901 (2002).
14. G. C. G. Berkhout, M. P. J. Lavery, J. Courtial, M. W. Beijersbergen, and M. J. Padgett, "Efficient sorting of orbital angular momentum states of light," Phys. Rev. Lett. **105**(15), 153601 (2010).
15. O. Bryngdahl, "Geometrical transformations in optics," J. Opt. Soc. Am. **64**(8), 1092–1099 (1974).
16. W. Hossack, A. Darling, and A. Dahdour, "Coordinate transformations with multiple computer-generated optical-elements," J. Mod. Opt. **34**, 1235–1250 (1987).
17. Y. Saito, S. Komatsu, and H. Ohzu, "Scale and rotation invariant real-time optical correlator using computer generated hologram," Opt. Commun. **47**(1), 8–11 (1983).
18. M. P. J. Lavery, G. C. G. Berkhout, J. Courtial, and M. J. Padgett, "Measurement of the light orbital angular momentum spectrum using an optical geometric transformation," J. Opt. **13**, 064006 (2011).
19. G. C. G. Berkhout, M. P. J. Lavery, M. W. Beijersbergen, and M. J. Padgett, "Measuring orbital angular momentum superpositions of light by mode transformation," Opt. Lett. **36**, 1863–1865 (2011).
20. T.A. Dow, M.H. Miller, and P.J. Falter, "Application of a fast tool servo fordiamond turning of non-rotationally symmetric surfaces," J. Precision Eng. **13**, 243–250 (1991).
21. C. E. Shannon, "A mathematical theory of communication," Bell Syst. Tech. J. **27**, 379 (1948).
22. M. J. Padgett and L. Allen, "The Poynting vector in Laguerre-Gaussian laser modes," Opt. Commun. **121**, 36–40 (1995).
23. J. Leach, S. Keen, M. J. Padgett, C. Saunter, and G. D. Love, "Direct measurement of the skew angle of the Poynting vector in a helically phased beam," Opt. Express **14** , 11919–11924 (2006).

The desire to increase the amount of information that can be encoded onto a single photon has driven research into many areas of optics. One such area is optical orbital angular momentum (OAM) [1]. The work by Allen *et al.* in 1992 showed that beams with an transverse amplitude profile of $A(r)\exp(i\ell\phi)$ carry an orbital angular momentum of $\ell\hbar$ per photon [1,2]. An example are Laguerre-Gaussian (LG) beams which have a helical phase structure, with r and ϕ as the radial and angular coordinates respectively. The integer ℓ is unbounded, giving a large state space in which to encode information [3–7].

The use of diffractive optical elements (DOEs) containing an ℓ-fold fork dislocation has become commonplace for the generation of beams carrying OAM [8, 9]. The forked diffraction grating, when illuminated with a Gaussian beam, for example from a single-mode fibre, produces the helical mode in the first diffraction order. This grating can also be used in reverse to couple light with a helical phase into a single-mode fibre, measuring the power in that mode [10]. Sequentially changing the dislocation in the fork allows a range of ℓ values to be measured, but checking for N states require at least N photons [10]. Similar techniques have been demonstrated using spiral phase plates and q-plate technology in place of the DOE [11,12]. A method to route OAM at the single photon level was demonstrated by Leach *et al*. It required a $N-1$ Mach-Zehnder interferometers with a Dove prism in each arm [13] for the routing of N states. In principle, this routing can be achieved with 100% efficiency and with no loss of the input beam's mode structure. However, simultaneously maintaining the alignment of N interferometers has proved technically challenging.

We recently showed that two diffractive optical elements, implemented on spatial light modulators (SLMs), can be used to transform OAM states into transverse momentum states [14]. This was achieved through the use of mapping of a position (x,y) in the input plane to a position (u,v) in the output plane, where $u=-a\ln(\sqrt{x^2+y^2}/b)$ and $v=a\arctan(y/x)$ [15–17]. A mapping of this type transforms a set of concentric rings at the input plane into a set of parallel lines in the output plane. The combination of the two diffractive optical elements transforms both the phase and intensity of the beam in the form $\exp(i\ell\phi)$, to give a complex amplitude at the output plane of the form $\exp(i\ell v/a)$. A lens can then separate the resulting transverse momentum states into specified lateral positions, allowing for the efficient measurement of multiple states simultaneously [18, 19]. In our previous proof-of-principle demonstration, approximately three

#153707 - $15.00 USD Received 1 Sep 2011; revised 10 Nov 2011; accepted 2 Dec 2011; published 17 Jan 2012

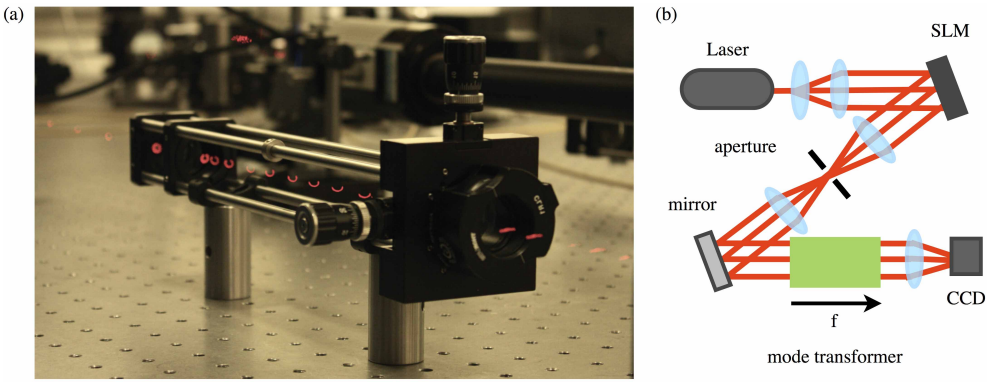

Fig. 1. (a) Conversion of OAM states into transverse momentum states with refractive optical elements. An image of the beam was captured in several transverse planes and overlaid (in red) to give the image shown above. (b) A beam carrying OAM is prepared through the use of a ℓ-forked hologram, realised using a spatial light modulator (SLM) and then passed through the two elements, represented as the green rectangle, required to perform the transformation of both the phase and intensity of the beam.

quarters of the input light was lost due to the limited diffraction efficiency of the SLMs [14].

In this paper we replace the previously used diffractive optical elements with refractive elements which carry out the desired optical transformation (Fig. 1). The transmission efficiency of the combination of elements is approximately 85%, which makes them attractive for use with single photons. The number of components was also reduced through the integration of the transform lens previously required between the diffractive optical elements into the transformation elements themselves. The height profiles for the refractive elements (Fig. 2) were derived from the equations defining the phase profile of the diffractive elements [14], along with the addition of a lens term, indicated in Eq. (1) and Eq. (2) shown below.

When light of a particular wavelength, λ, passes through a material of height Z, and with a refractive index n, the effective optical path length changes with respect to the same distance of propagation in a vacuum. The change in path length can be expressed as a change in phase of $\Delta\Phi = 2\pi(n-1)Z/\lambda$, hence the first element requires a height profile of

$$Z_1(x,y) = \frac{a}{f(n-1)}\left[y\arctan\left(\frac{y}{x}\right) - x\ln\left(\frac{\sqrt{x^2+y^2}}{b}\right) + x - \frac{1}{a}\underbrace{\left(\frac{1}{2}(x^2+y^2)\right)}_{\textit{lens term}}\right], \qquad (1)$$

where f is the focal length of the integrated lens. There are two free parameters, a and b, which determine the scaling and position of the transformed beam. The parameter a takes the value $a = d/2\pi$, ensuring that the azimuthal angle range $(0 \mapsto 2\pi)$ is mapped onto the full width of the second element, d. The parameter b is optimised for the particular physical dimensions of the sorter. The second of these elements has a height profile

$$Z_2(x,y) = -\frac{ab}{f(n-1)}\left[\exp\left(-\frac{u}{a}\right)\cos\left(\frac{v}{a}\right) - \frac{1}{ab}\underbrace{\left(\frac{1}{2}(u^2+v^2)\right)}_{\textit{lens term}}\right], \qquad (2)$$

#153707 - $15.00 USD Received 1 Sep 2011; revised 10 Nov 2011; accepted 2 Dec 2011; published 17 Jan 2012

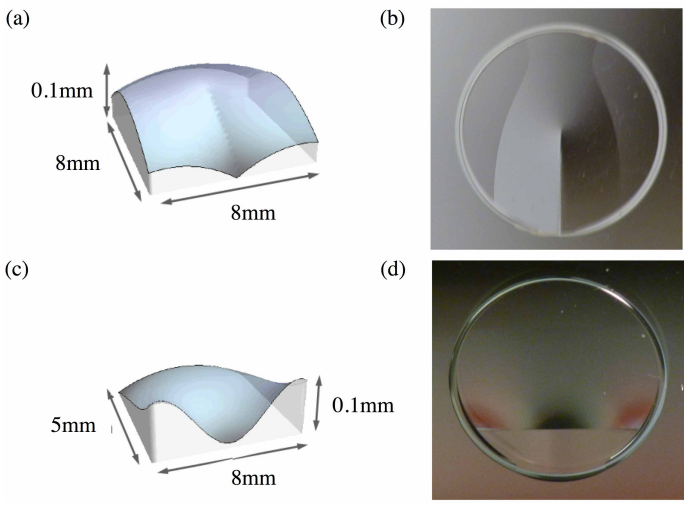

Fig. 2. Height profiles (a,c) and photos (b,d) of refractive elements 1 (top) and 2 (bottom). The aperture size is $d = 8$mm, focal length $f = 300$mm and the parameter $b = 0.00477$. The surfaces were made from PMMA (Poly methyl methacrylate), using a machined radius of 5.64 mm, angular spacing 1°, radial spacing of 5 μm, spindle speed of 500 RPM, roughing feedrate 5 mm/minute with a cut depth of 20 μm and finishing feedrate 1 mm/minute with a cut depth of 10 μm [20].

where u and v are the coordinates in the output plane. This element is placed a distance f behind the first element. Each surface is wavelength independent, but dispersion effects in the material manifest themselves as a change in the focal length of the integrated lens for different wavelengths. Hence, the system can be tuned to a specific wavelength by changing the distance between the elements.

The elements were diamond machined using a Natotech, 3 axis (X,Z,C) ultra precision lathe (UPL) in combination with a Nanotech NFTS6000 fast tool servo (FTS) system to provide a fast (W) axis superimposed on the machine Z-axis. The machining programme was generated using proprietary code written within commercially available software, DIFFSYS. This programme converts the input data, in the form of an X,Y,Z cloud of points, into the requisite UPL machine and FTS system machining files.

Generally, when machining freeform surfaces it is normal to separate out the symmetrical and non-symmetrical components to realise minimum departure, of the FTS tool and therefore maximise machining performance [20]. However, as the total sag height difference for each part was relatively small (115um for surface 1 and 144um for surface 2) and as both surfaces are highly asymmetric resulting in a small component of symmetric departure the elements were machined using FTS tool movement in W only. The surfaces are shown in Fig. 2(b) and 2(d).

In our experiment we generate Laguerre-Gaussian (LG) beams by expanding a HeNe laser onto a ℓ-forked hologram, realised using a SLM, by programming the SLM with both phase and intensity information. The beam generated in the first order of the hologram was selected with an aperture and the plane of the SLM is imaged onto the plane of the first element. The beam is then passed through the elements transforming it into the form $\exp(i\ell v/a)$, giving a transverse direction state which is then focussed into an elongated spot on a camera. The transverse position of the spot is dependent on ℓ.

An important consideration in any communication system is the cross talk between the channels in that system. To assess this the camera was portioned into N adjacent regions, where each

#153707 - $15.00 USD Received 1 Sep 2011; revised 10 Nov 2011; accepted 2 Dec 2011; published 17 Jan 2012

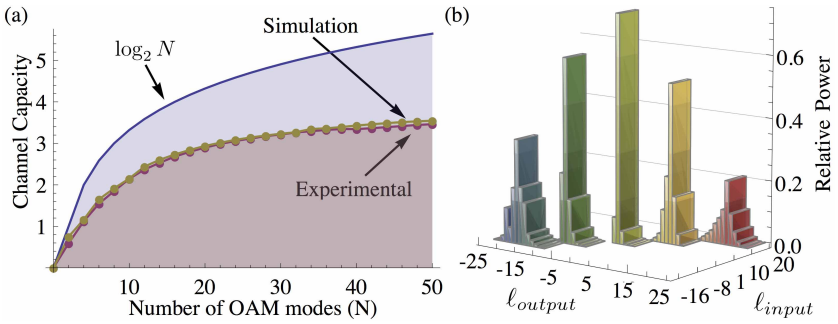

Fig. 3. (a) Channel capacity for a N of LG modes, where $N = 2,4,6,...,50$. Detector noise was measured with no light incident on the camera, which was overcome by setting a threshold with a signal to noise ratio of 3000 to 1. (b) The ratio of energy measured in each of the detector regions showing the degree of cross talk.

region is centred on one elongated spot, and the measured intensity of the pixels in the region was summed for each region. For a single input mode, one would expect the majority of the energy to be detected in the bin corresponding to the input mode and any energy readings in other regions represent cross talk between channels. Our transformation from orbital angular momentum states into transverse momentum states gives rise to inherent cross talk due to the diffraction limit. The inherent degree of cross talk can be deduced from Fourier theory, which predicts approximately 80% of the input light will be present in the bin corresponding to that input OAM mode value. A common method of evaluating the degree of cross talk in a communications system is the channel capacity, which is the maximum amount of information that can be reliably transmitted by an information carrier [21]. In a multi-channel system, a photon can be in one of N input states and the maximum channel capacity value is $\log_2 N$ bits per photon.

To evaluate the range of modes the system is able to detect efficiently, the system is tested using LG beams over the mode range $\ell = -25$ to $\ell = 25$. The choice of LG beams allows the beam waist to be controlled, and the experimental result to be very closely matched to numerical modelling of the system. The channel capacity was measured for N modes, where $N = 2,4,6,...,50$. For each measurement the range $\ell = -N/2$ to $\ell = N/2$ was used while leaving $\ell = 0$ free as an alignment channel. The values measured are shown in Fig. 3. The optical transformation we utilise is only perfect for rays which are normally incident on the transformation elements. Helically phased beams are inherently not of this type, and have a skew angle of the rays of $\theta_s = \ell/kr$, where k is the wavenumber of the light and r is the distance from the beam centre [22,23]. A numerical simulation of the experimental setup was carried out using plane wave decomposition [14]. Comparing channel capacity values from the simulated and experimentally obtained results, with that of the maximum possible channel capacity, one sees the difference increase at higher mode ranges. These results are consistent with the larger skew angle at higher ℓ causing errors in the transformation, hence increasing the channel cross talk at these ℓ values. Simulations show that reducing the separation between the components or increasing the aperture size of the system can reduce these skew angle effects at higher ℓ values, hence reducing the cross talk within the system.

The optical efficiency of the transformation elements is very important for the use of such a technique within quantum communications. To test that our transformation elements are adequately efficient for use with single photons, we replace the standard camera with an electron multiplying CCD (EMCCD) camera which is sensitive to single photons. The power of the input beam before the first element was attenuated to a power of approximately 2×10^{-17} W,

#153707 - $15.00 USD Received 1 Sep 2011; revised 10 Nov 2011; accepted 2 Dec 2011; published 17 Jan 2012

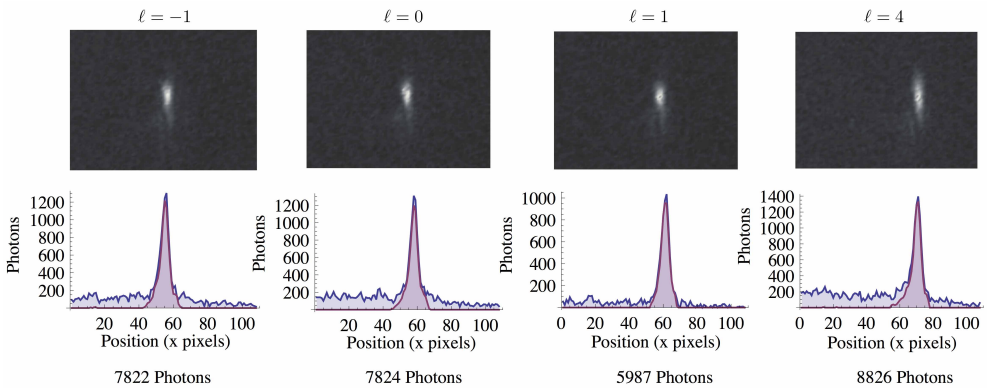

Fig. 4. Using a EMCCD camera in single photon counting mode, images were generated by summing over 16383 frames. Each pixel has a dark count rate, generating noise on every pixels in the camera. The images is shown are the raw captured images. The dark count rate was assessed by counting the photons over the same capture period with the camera shutter closed. A threshold was set with a value corresponding to the mean, plus one standard deviation of the dark count rate. The corresponding graph is a some of each column, in blue, and superimposed with the results when a Wiener Noise reduction filter is applied shown in red. Summing under the red curve gives us an approximation of the number of photons received at the camera plane.

corresponding to approximately 75 photons per second entering the first element. The camera was set to capture 100 frames per second, hence on average we record less than one photon per measurement.

To verify that our measurement corresponds to the expected number of photons, we first measure the unattenuated power before entering the first element and at the camera plane giving a measured efficiency of approximately 75%, 10% lower then the combination of transformation elements. This difference arises from the losses due to scatter of the other optical components. The efficiency could be further improved by adding anti-reflective coating to the elements. A measurement of the efficiency at the level of single photons was made by counting the number of photons detected over a large number of accumulated camera frames when used in single photon counting mode. The images produced are shown in Fig. 4. The quantum efficiency of the entire system (including the effects of all optical components and the efficiency of the EMCCD camera) was measured to be approximately 50%.

In conclusion, we have developed a mode transformer comprising two refractive elements which can separate beams carrying OAM into discrete regions on a detector with an efficiency of 85%. In the case of many photons, the experimental system was characterised to have a channel capacity for 8 modes of 1.85 bits per photon, 16 modes of 2.68 bits per photon and for 32 modes of 3.26 bits per photon. An attenuated laser source, where on average there was less then one photon in the system within any measurement period, demonstrates the elements are capable of separating the OAM states of the input light at the level of single photons. This approach could be used to generate and detect OAM states used within quantum communications or quantum key distribution systems, increasing the amount of information one can encode onto a single photon.

We acknowledge Robert W. Boyd, Daniel J. Gauthier, Mehul Malik and Brandon Rodenburg for helpful discussions. M. J. P. is supported by the Royal Society. Our work was supported by EPRSC, the DARPA InPho program through the US Army Research Office award W911NF-10-1-0395 and as part of the European collaboration EC FP7 255914, PHORBITECH.

#153707 - $15.00 USD Received 1 Sep 2011; revised 10 Nov 2011; accepted 2 Dec 2011; published 17 Jan 2012